A fossil chrysochlorid skull in the Ditsong National Museum of Natural History: Robert Broom's missing specimen unearthed?

Matthew J. Mason[1*][§], **Nigel C. Bennett**[2] **& Martin Pickford**[3]

[1]*Department of Physiology, Development & Neuroscience, University of Cambridge, Downing Street,*
Cambridge CB2 3EG, United Kingdom
[2]*Department of Zoology and Entomology, University of Pretoria, Pretoria, 0002 South Africa*
[3]*Sorbonne Université, CR2P, MNHN, CNRS, UPMC, Paris VI, France*

Received 4 December 2018. Accepted 8 April 2019

An unlabelled, fossilized skull of a golden mole from the Ditsong National Museum of Natural History, Pretoria, was examined through micro-computed tomography. Reconstructions show that the species in question has alveoli for nine teeth in each upper jaw, although only six teeth in total remain. The skull resembles those of the extant chrysochlorids *Amblysomus* and *Calcochloris*, which also have nine teeth, but in most respects it is closer to *Amblysomus*. The ear region, examined in detail, also proved to be very similar to that of *Amblysomus*. Damage to the teeth and palate are consistent with the brief descriptions of a fossil golden mole skull first mentioned by Robert Broom in 1948. This specimen, dating from the Plio-Pleistocene and provisionally identified as *Proamblysomus antiquus*, subsequently went missing. We argue that the skull described here is Broom's lost specimen, but whether this fossil species really deserves generic distinction from extant groups remains unclear.

Keywords: golden mole, Chrysochloridae, Afrotheria, *Proamblysomus*, inner ear, malleus.

INTRODUCTION

While studying fossil suids from the Gauteng karst system curated at the Ditsong National Museum of Natural History in Pretoria in October 2017, M.P. found the unlabelled, fossilized skull of a chrysochlorid lying loose in a tray of bones and teeth. The tray lacked any indication of the locality from whence these specimens came, but the rear part of a juvenile right mandible with the distal part of a first molar fits onto SK 380, a specimen of the extinct suid *Phacochoerus modestus* Van Hoepen & Van Hoepen (1932), from Swartkrans. There is no guarantee, however, that all the specimens in the tray came from this locality.

The chrysochlorid skull (Fig. 1A,C) lacks mandibles, but appeared from visual inspection to be reasonably well-preserved. The dorsal surface, both zygomatic arches and much of the occiput were exposed and visible from a dorsal view (Fig. 1A). Sediment covering much of the ventral part of the skull had evidently been smoothly ground off with a rotating abrasive wheel. Several teeth had been exposed and cut through in this process, most obviously including the first incisors and a right premolar, and an opening had been made into the right auditory bulla (Fig. 1C). Also exposed, but apparently not cut through by the wheel, were the right occipital condyle and some of the hard palate. What remains of the exposed palate has a creamy white colour in Fig. 1C but the posterior part is missing, revealing the reddish matrix within the nasal cavity.

Several chrysochlorid skulls from the Gauteng karst deposits have been noted in the literature. Renowned palaeontologist Robert Broom briefly described two specimens from the caves of Sterkfontein, one the holotype of *Proamblysomus antiquus* from 'Mr Bolt's workings', the other the holotype of *Chlorotalpa spelea*, from the same cave that yielded the type specimen of *Plesianthropus transvaalensis* (Broom, 1941). In 1948, Broom alluded to the discovery of a third Plio-Pleistocene chrysochlorid skull from Kromdraai. No picture was provided: his remarks about this skull were only that 'It has a number of teeth well preserved. It is allied to, and possibly belongs to, the species *Proamblysomus antiquus*; but as the teeth of this are unknown it is impossible at present to be quite sure of the identity.' De Graaff (1958) mentioned the same specimen, referring to the 'damaged condition of the palate and the teeth'. He later assigned it to *P. antiquus* (De Graaff 1961). In 2010, Asher lamented that this specimen 'frustratingly, now appears to be lost'.

The existence of a fourth chrysochlorid skull from the Gauteng deposits was mentioned by Asher (2010) with the words 'The type of *C. spelea* (TM 1572) preserves only the right P2 but shows alveoli for 10 teeth in each quadrant. A third fossil golden mole skull kept with the *C. spelea* type in the TM collections (TM 1572-327) most likely has

---

[*]Author for correspondence. E-mail: mjm68@hermes.cam.ac.uk

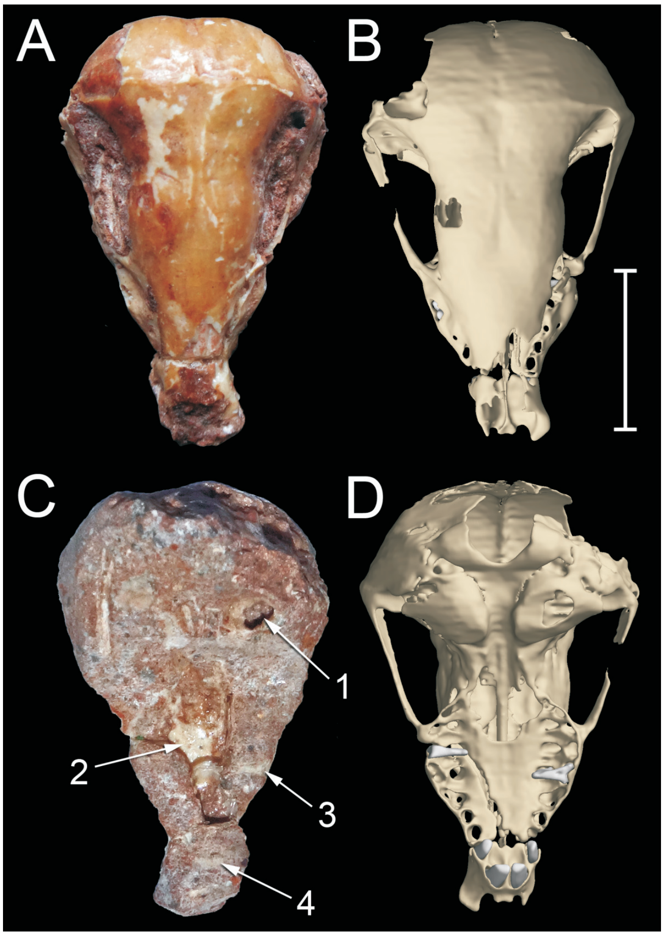

Figure 1. The fossil golden mole skull in the Ditsong National Museum of Natural History. **A**, **C**, Photographs of the skull, partially embedded in matrix, in dorsal and ventral views, respectively. **B**, **D**, Reconstructions of the same skull based on CT scans, also in dorsal and ventral views, respectively. 1 = right bulla, broken open; 2 = exposed hard palate; 3 = exposed right premolar; 4 = exposed incisors. Scale bar 10 mm.

only nine alveoli'. Golden mole specimens assigned to *Chlorotalpa*, *Chrysospalax* and an undescribed new chrysochlorid genus were listed by Pocock (1987) as coming from Kromdraai and Sterkfontein. No further information was given about the nature of these specimens. Avery (1998, 2000) briefly discussed material attributed to *Chlorotalpa*, *Chrysospalax* and *Neamblysomus* species from the Pleistocene of Sterkfontein and Swartkrans, but only mentioned mandibles and one maxilla.

Another fossil chrysochlorid was described from Makapansgat, originally named *Chrysotricha hamiltoni* (De Graaff 1958). '*Chrysotricha*' is a junior synonym of *Calcochloris*, the extant genus which De Graaff believed his fossil skull was closest to, based on its high width:length index. However, this specimen has subsequently been considered to be a species of *Amblysomus* (Asher 2010; Butler 1978).

We contend that the unlabelled fossil skull in the Ditsong National Museum of Natural History represents Broom's missing specimen, first mentioned in 1948 and suspected to be a species of the extinct genus *Proamblysomus*. Broom's original description of *Proamblysomus antiquus* in 1941 was very brief, forming just one part of a two-sided paper. The holotype skull lacked the anterior snout and retained no teeth, and was crudely illustrated in dorsal view. A photograph of that specimen (Ditsong National Museum of Natural History TM PAL 1573) in ventral view was presented by Asher (2010), but no further details were provided. If the specimen examined in the present study is indeed a *Proamblysomus*, the description presented herein represents the most comprehensive account to date of a skull of this genus.

MATERIALS AND METHODS

Two CT scans were made of the fossil in the University of Cambridge Biotomography Centre, using a Nikon XT H 225 CT-scanner. One scan included the whole specimen, while the second was a close-up of the posterior skull, including the ear region. 1080 projections were taken each time with 1 second exposure per frame and two frames averaged per projection, using settings of 125 kV and 120 μA. Tomograms were constructed using CT Agent XT 3.1.9 and CT Pro 3D XT 3.1.9 (Nikon Metrology, 2004-13). Cubic voxel side-lengths were 15 μm (whole specimen) and 10 μm (posterior skull). We also scanned one ethanol-preserved head of a male *Amblysomus hottentotus*, which had been collected in San Lameer, Natal, South Africa, under permit from Ezemvelo Nature Conservation, KwaZulu-Natal. Scans were made of the whole head and then the right ear region was dissected out and separately scanned. Settings of 170 kV and 170 μA were used; cubic voxel side-lengths were 16 μm (head) and 7.5 μm (ear). All *Amblysomus* reconstructions shown in this paper were made from this specimen. For comparative purposes, scans recently made by the same team in a very similar way (Mason *et al*. 2018) were available for two further *Amblysomus* specimens which had been collected together with the specimen described above, plus two specimens of *Calcochloris obtusirostris* from The Natural History Museum, London (BMNH 1906.11.8.25 and 1906.11.8.26). Although *Neamblysomus* species were not directly examined as part of this study, photographs and measurements of one specimen of *N. gunningi* (BMNH 51.299) and one of *N. julianae* (TM 39770), made as part of previous studies, were consulted.

The raw tomogram files were loaded into ImageJ 1.52b (Wayne Rasband, National Institutes of Health, U.S.A.), which ran a Contrast-Limited Adaptive Histogram Equalization (CLAHE), using the ImageJ plugin developed by Stephan Saalfeld. Through enhancing local contrast, CLAHE made it easier to distinguish fossilized bone from matrix. Files were then saved as 8-bit JPG files and 3D reconstructions of the fossil skull were made from the enhanced images using Stradwin 5.3 (Graham Treece, Andrew Gee & Richard Prager, 2017). This involved manually identifying the boundaries of the structures of interest. The delicate turbinate bones within the nasal cavity were preserved, but not modelled. Within the middle ear cavity, the positions of arteries, facial nerve and stapedius muscle belly were inferred from the bony tubes that surrounded them.

To make skull reconstructions from scans of *Amblysomus* and *Calcochloris*, tomogram images were converted to 8-bit JPG files and in some cases reduced in size, then loaded into Microview 2.5.0 (Parallax Innovations Inc.

2018). Where necessary, mandible, hyoid apparatus and teeth were digitally removed from the tomograms using Adobe Photoshop CS 8.0 (Adobe Systems Inc. 2003). Ear structures were reconstructed using Stradwin, as above.

Measurements were made from the 3D reconstructions. Following Bronner (1995), greatest skull length was measured from the rostral-most premaxilla to the most posterior part of the occiput, greatest skull height was measured between the base of the occipital condyles and the highest point on the skull in the midline, greatest skull width was measured between the zygomatic processes of the squamosals, and mid-interorbital width was measured as the greatest width across the frontals in the interorbital region. Because of damage to the fossil specimen, the greatest skull length was in this case measured from the posterior occiput, which was slightly compressed inwards, to the tip of the left premaxilla, the right one being broken off.

RESULTS

CT reconstructions reveal that much of the fossil skull is intact, but there is extensive damage to the right occipital and temporal regions (Figs 1B,D; 2C,D & 3C,D). The distal snout and left maxilla are both detached from the rest of the skull but remain very close to their natural positions, by comparison with extant golden mole skulls (Figs 2 & 3). The right narial flange and the dorsal snout are damaged. The delicate turbinate bones within the nasal cavity are intact, the air-spaces between them being only partly filled by matrix. A comparison of the hard palate in the fossil reconstruction (Fig. 2D) with that of extant golden moles (Fig. 2B,F) confirms that its posterior part is missing.

The fossil skull is wedge-shaped in dorsal view (Figs 1B & 2C), broad posteriorly at the brain case, narrowing anteriorly to the level of the second incisor before flaring laterally at the external nares where the narial flange, intact on the left side only, forms a prominent feature. What remains of the snout has steep sides and a rounded dorsal profile. The posterior half of the braincase has a bulbous appearance, with a shallow central furrow running posteriorly from the nuchal crest downwards towards the foramen magnum. The transverse nuchal crest is almost rectilinear, running across the broadest part of the skull between the distal ends of the zygomatic arches. The anterior half of the braincase has two clear temporal lines that are about 4.5 mm apart where they join the nuchal crest. The temporal lines converge anteriorly but do not fuse to form a sagittal crest, instead remaining separated

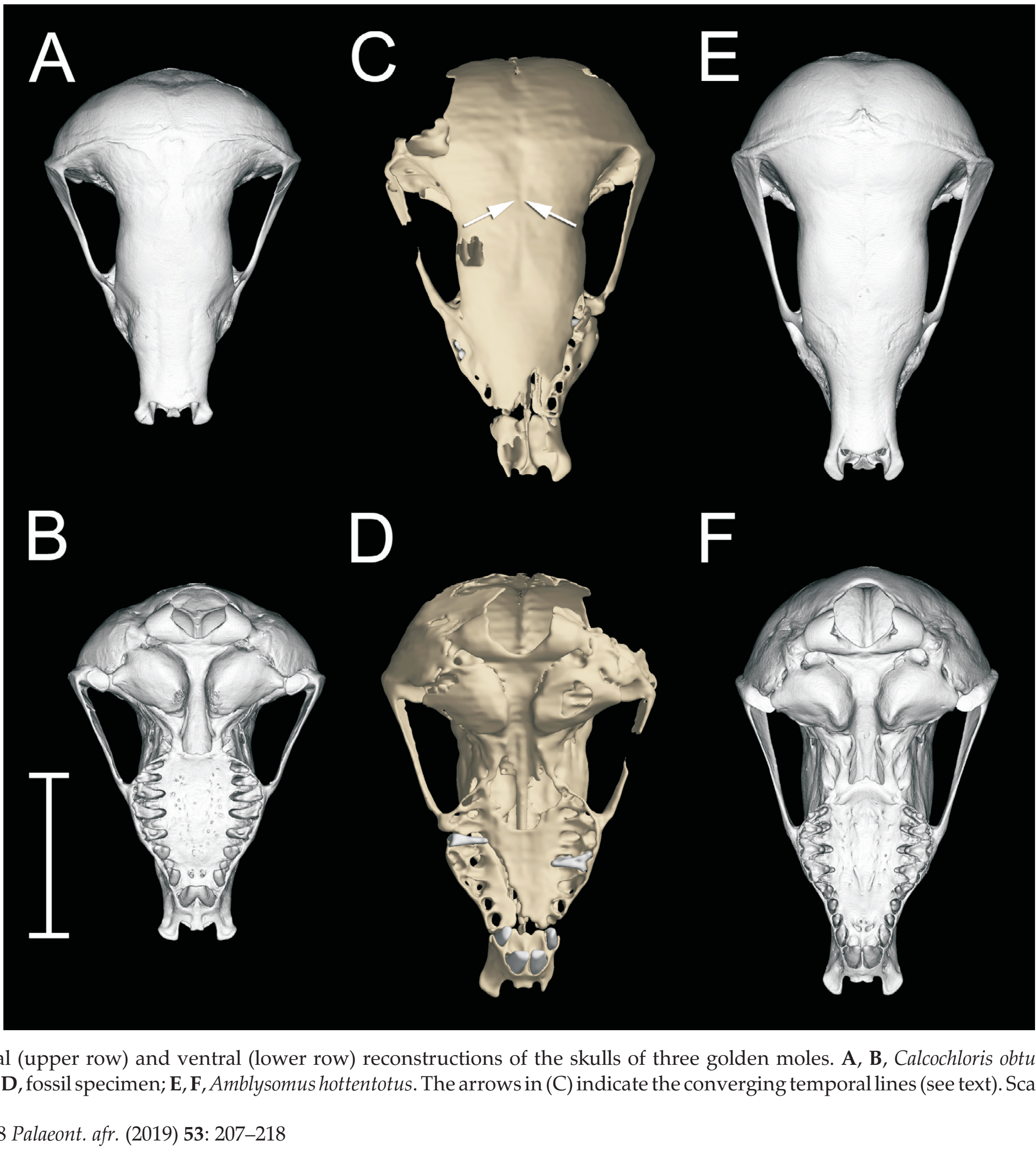

Figure 2. Dorsal (upper row) and ventral (lower row) reconstructions of the skulls of three golden moles. **A**, **B**, *Calcochloris obtusirostris* BMNH 1906.11.8.26; **C**, **D**, fossil specimen; **E**, **F**, *Amblysomus hottentotus*. The arrows in (C) indicate the converging temporal lines (see text). Scale bar 10 mm.

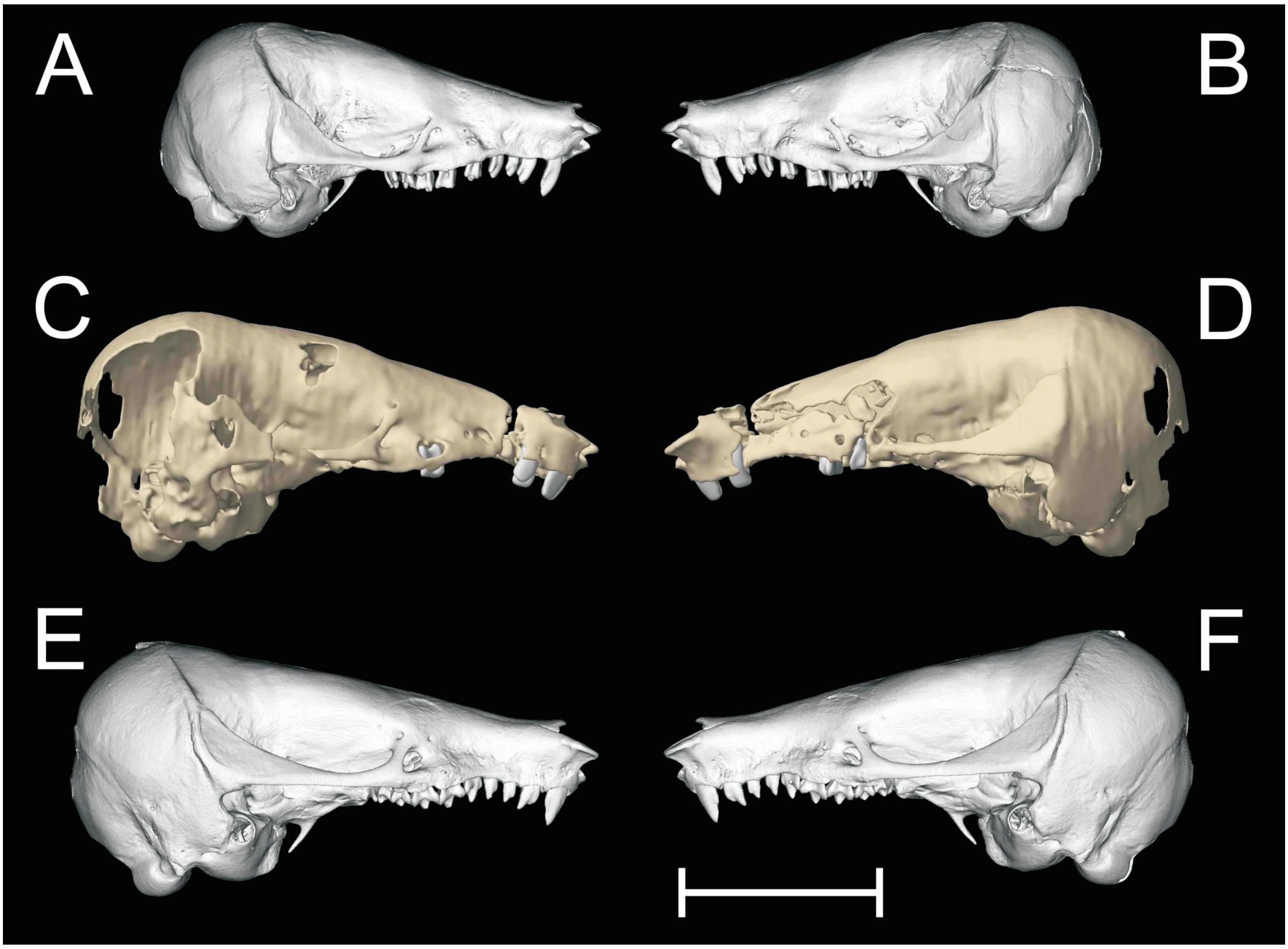

Figure 3. Reconstructions of the skulls of three golden moles in lateral views. **A**, **B**, *Calcochloris obtusirostris* BMNH 1906.11.8.26; **C**, **D**, fossil specimen; **E**, **F**, *Amblysomus hottentotus*. Scale bar 10 mm.

from each other by a shallow groove about 1 mm wide (Fig. 2C). They run parallel to each other before diverging and fading out above the orbits.

The orbits are confluent with the temporal fossa, with only a subtle post-orbital swelling along the dorsal margin showing the boundary zone between the two. The zygomatic arch (Fig. 3C,D) extends from the base of the orbit anteriorly, where it is narrow (*c*. 0.6 mm), to the nuchal crest, where it is taller (*c*. 4 mm). In dorsal view the zygomatic arches are extremely slender, as in most chrysochlorids. The infra-orbital foramen is located immediately anterior to the leading edge of the orbit, being separated from it by a sliver of bone that slants anteriorly as it rises from above the tooth row. It opens low down on the maxilla just over 1 mm in front of the leading edge of the orbit. There is a wide division between the foramen ovale and the sphenorbital fissure, several times the diameter of the foramen ovale.

Measurements made from the skull reconstructions are presented in Table 1.

Table 1. Measurements of the fossil skull, taken from CT reconstructions.

Anatomy	Measurement (mm)
Greatest skull length	26.6
Greatest skull height	12.7
Greatest skull width	17.2
Mid-interorbital width	8.3
Distance between occiput and infra-orbital foramen	16.5

Dentition

There are alveoli for nine teeth in each upper jaw of the fossil examined (Fig. 4). The meristic homologies of the teeth in golden moles are unclear. Some authors have regarded the fifth tooth from the front, which is molariform in *Calcochloris* but typically triconid and sectorial in *Amblysomus*, to be P^1 (Bronner 1995, 1996b; Meester 1974; Skinner & Smithers 1990). However, the deciduous P^1 is rarely replaced in eutherians (Luckett 1993), in which case the first successional premolar in golden moles would likely be P^2. O'Leary *et al*. (2013) contend that the primitive dentition for placental mammals lacks P^3, suggesting that the three successional premolars in a typical species might be P^2, P^4 and P^5. Because our data add nothing to this debate, which is further complicated by the late eruption of successional teeth in golden moles (Asher & Lehmann 2008), we will refer simply to the first (PM1), second (PM2) and third (PM3) premolars, without making any claims about homology with other species. We follow previous authors (Asher *et al*. 2010; Bronner 1995, 1996b; Meester 1974; Skinner & Smithers 1990) in taking the posterior two teeth in golden moles with nine teeth in each upper jaw to be molars, which we refer to as M1 and M2, thus assuming an upper dental formula of 3132 for our fossil.

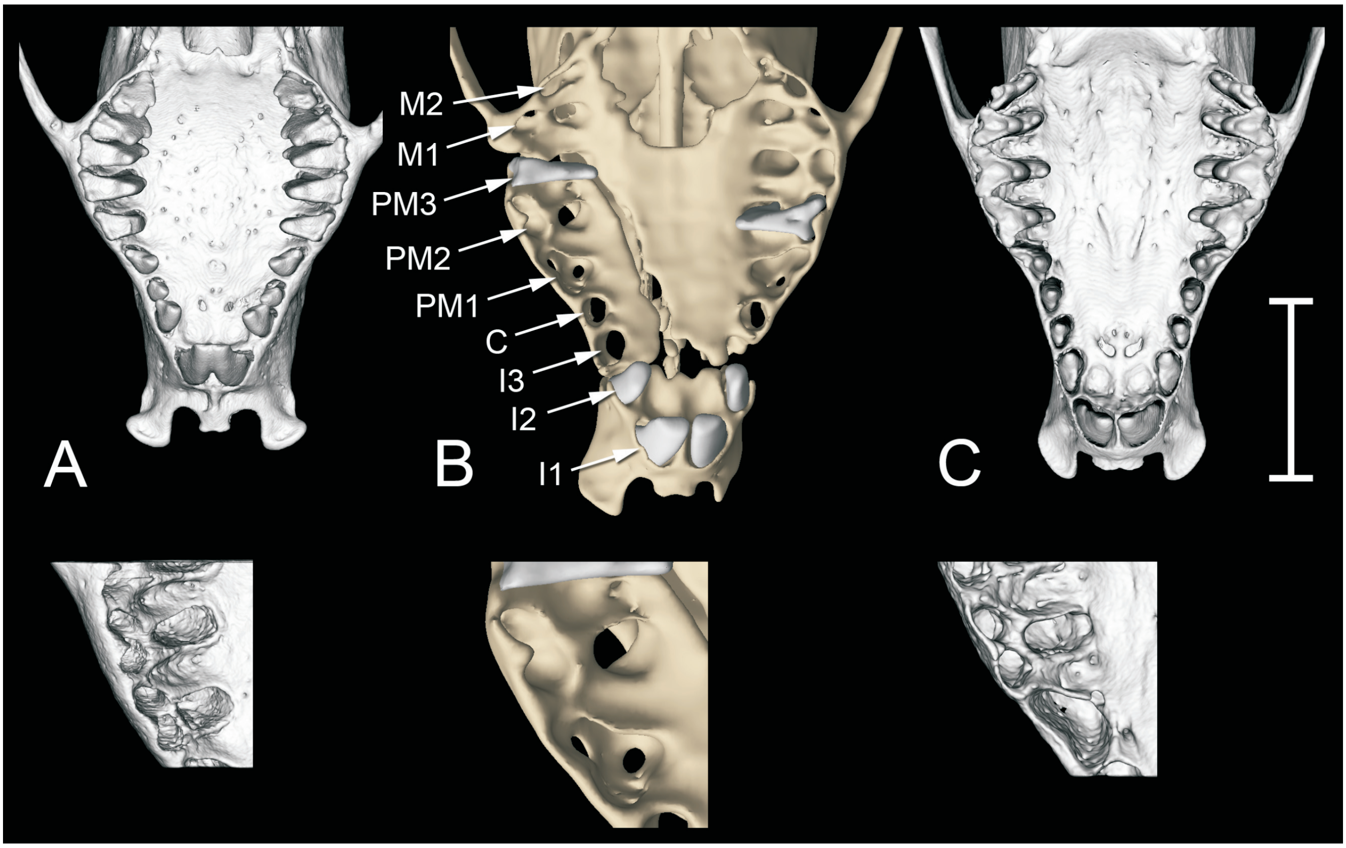

Figure 4. Reconstructions of the upper jaws and snout regions of (**A**) *Calcochloris obtusirostris* BMNH 6.11.8.25, (**B**) fossil specimen, with the positions of each of the nine teeth indicated, and (**C**) *Amblysomus hottentotus*. Below each reconstruction is a ×2 close-up of the alveoli for the first and second left premolars (the teeth were digitally removed from the scans of *Amblysomus* and *Calcochloris*). Teeth or alveoli are labelled as C = canine, I = incisor, M = molar, PM = premolar, followed by numbers indicating only the positional order in the jaw (see text). Scale bar for upper row 5 mm, for lower row 2.5 mm.

Six teeth are retained in the fossil specimen: the first and second incisors on each side, the second premolar on the right side and the third premolar on the left side (Fig. 4B). The crowns of the premolars have been damaged in preparation, but it is clear that both teeth are zalambdodont and they appear to possess small protocones. These teeth are narrow rostro-caudally.

The upper central incisors, significantly larger than the second incisors, resemble curved pillars with a rounded triangular section. They are oriented in the premaxilla such that the crown apices are slightly distal to the cervix (opisthodont). The two teeth are slightly separated at the cervices but touch each other apically. There is a short gap between first and second incisors. The latter tooth is vertically implanted in the jaw with a slight rearward curve of the apex. Behind the second incisor there are two ovoid alveoli, the anterior one slightly larger than the posterior one. These we take to be for a third incisor and canine, respectively, based on a comparison with extant chrysochlorids. There then comes the alveolus for PM1, which has a rounded triangular outline with three depressions corresponding to three roots. The molariform PM2 has a large lingual alveolus and two small, adjacent buccal alveoli. The alveoli for PM3 and M1 each comprise a prominent lingual alveolus and confluent buccal alveoli. The smaller alveolus for M2 is ovoid, barely separable into lingual and buccal depressions.

The lingual edges of the maxillary dental alveoli are arranged almost in straight lines, the left and right lines diverging gently to the rear. In contrast, the buccal alveoli are arranged in semi-circles. The lingual alveoli are separated from each other by relatively broad spaces, those between PM2 and PM3, and between PM3 and M1, having a depression in them. This is characteristic of chrysochlorids, the spaces between the successive upper teeth accepting the corresponding trigonids of the lower teeth when the jaws are closed.

Ear region

Each auditory bulla tapers laterally to end in a relatively narrow, circular bony meatus. A deep basicranial channel separates their medial borders. As mentioned above, the ventral wall of the right bulla has been broken to leave a hole penetrating into the middle ear cavity. There is some damage to the lateral part of the left bulla, around the bony meatus.

The basicranial bones are extensively pneumatized by extensions of the middle ear cavity (Figs 5 & 6). Most of this pneumatized region is trabeculated and spongy in appearance; some has been filled in with matrix while other areas remain air-filled. The basisphenoid bone contains trabeculae but there is no complete vertical septum, and as a result the right and left middle ear cavities clearly intercommunicate. The pneumatized zone extends into the posterior root of the zygomatic arch but it does not extend dorsal to the zygomatic root, nor does it extend into the occipital condyles (Fig. 5).

The middle ear ossicles are present and intact in the

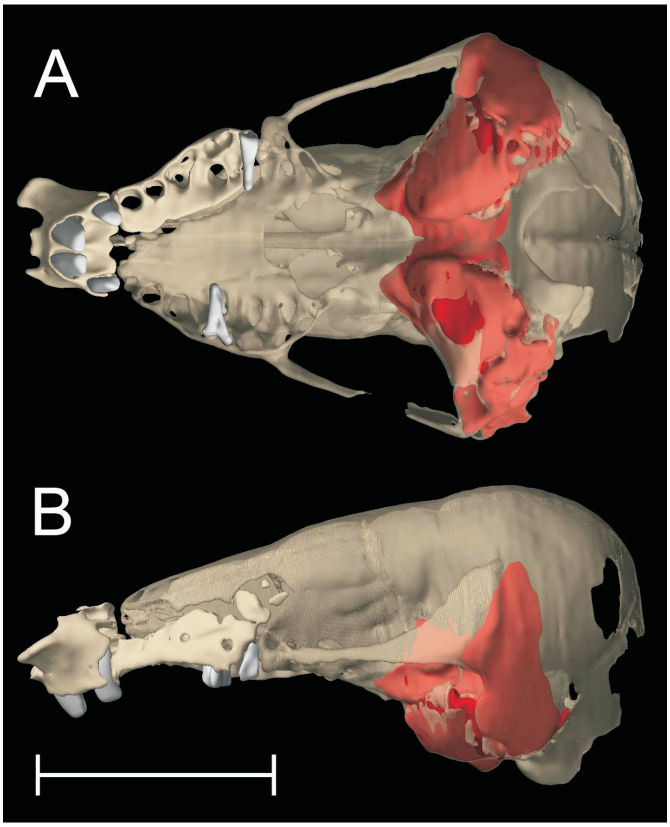

Figure 5. Reconstruction of the skull of the fossil specimen in (**A**) ventral and (**B**) left lateral views, with the main part of the skull shown semi-translucent. The extent of the middle ear cavity and associated pneumatization of the surrounding bones is indicated in red. Scale bar 10 mm.

fossil, although they have become disarticulated on both sides (Fig. 7A,G). Being relatively small, there is no expansion of the epitympanic recess, which accommodates the malleus head, into the orbit. The ossicles are very similar in morphology to those of *Amblysomus* (Fig. 7H), but the malleus is slightly bulkier in the fossil species. Its manubrium appears less spatulate than in *Amblysomus* and its anterior process is abbreviated, but these delicate processes may well have been damaged. The incus in the fossil has relatively slimmer processes. The stapes has a broad footplate; the bases of the crura appear to be damaged, on both sides. An intact, bony tube for the stapedial artery passes through the stapes in both the fossil and the *Amblysomus* specimen (Fig. 7A,B). From inspection of the bony canals, the inferior ramus of the stapedial artery seems to exit the skull through the foramen ovale in the fossil, rather than through a separate, adjacent opening. A bony tube for the stapedius muscle belly is present, merging rostrally with the tube for the facial nerve. However, there is no fossa for a tensor tympani muscle between stapedial and promontorial arteries.

The left bony labyrinth is intact in the fossil (Fig. 7C,E), but on the right side the posterior semicircular canal has been damaged. The anterior semicircular canal of *Amblysomus* (Fig. 7D,F) is relatively taller than in the fossil specimen, but otherwise the bony labyrinths are very similar. Both possess a secondary common crus formed from the fusion of lateral and posterior semicircular canals, and in neither case was a canaliculus cochleae for the perilymphatic duct identifiable. The cochleae have somewhere between 3 and 3.25 turns.

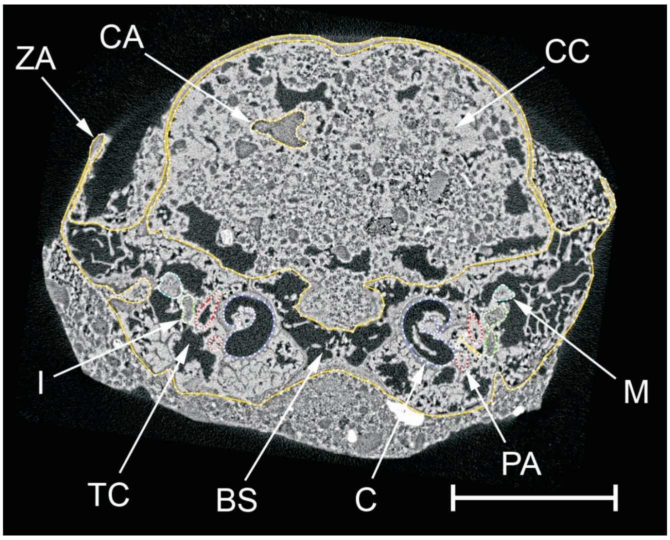

Figure 6. Contrast-enhanced tomogram section through the posterior part of the skull of the fossil specimen, in an approximately transverse plane. Much of the basicranium and the roots of the zygomatic arches consist of spongy bone pneumatized by extensions of the middle ear cavity. Features of interest have been outlined. BS = pneumatized basisphenoid; C = cochlea; CA = calcaneum; CC = cranial cavity, filled with matrix; I = incus; M = malleus; PA = bony tube for the promontorial artery (immediately above this is the stapes, and above that is the tube for the stapedial artery); TC = tympanic cavity; ZA = zygomatic arch. Scale bar 5 mm.

Additional material

At least sixteen additional bones and teeth were identified in the matrix within which the fossil skull was embedded, mainly within the cranial cavity (Fig. 6). The most identifiable include a calcaneum, talus, caudal vertebra and a cheek tooth (Fig. 8). The calcaneum (Fig. 8C) is from a rodent, as shown by the proximo-distally elongated shape and central position of the ectal facet, the laterally-flaring sustentaculum, the rounded, distal-facing calcaneo-cuboid facet and the elongated neck of the tuber calcanei, which is almost as broad as the articular parts (Ginot *et al*. 2016). The calcaneum of chrysochlorids has a small, globular ectal facet, and a short tuber calcanei which is appreciably narrower than the articular part (Pickford 2015). The talus (Fig. 8D) belongs to a chrysochlorid, as shown by the shallow trochlear groove, the extremely short neck and diminutive head (Pickford 2015), which contrasts with the deeper groove and the expanded head and neck in rodents (Ginot *et al*. 2016). The tooth (Fig. 8B) is the upper right first molar of a rodent, probably *Steatomys*.

DISCUSSION

Evidence that this was Broom's missing specimen

It can never be proven conclusively that the specimen described here is indeed the missing Kromdraai specimen, first mentioned by Robert Broom in 1948, referred to by De Graaff a decade later, and subsequently reported to be lost (Asher 2010). However, the following points

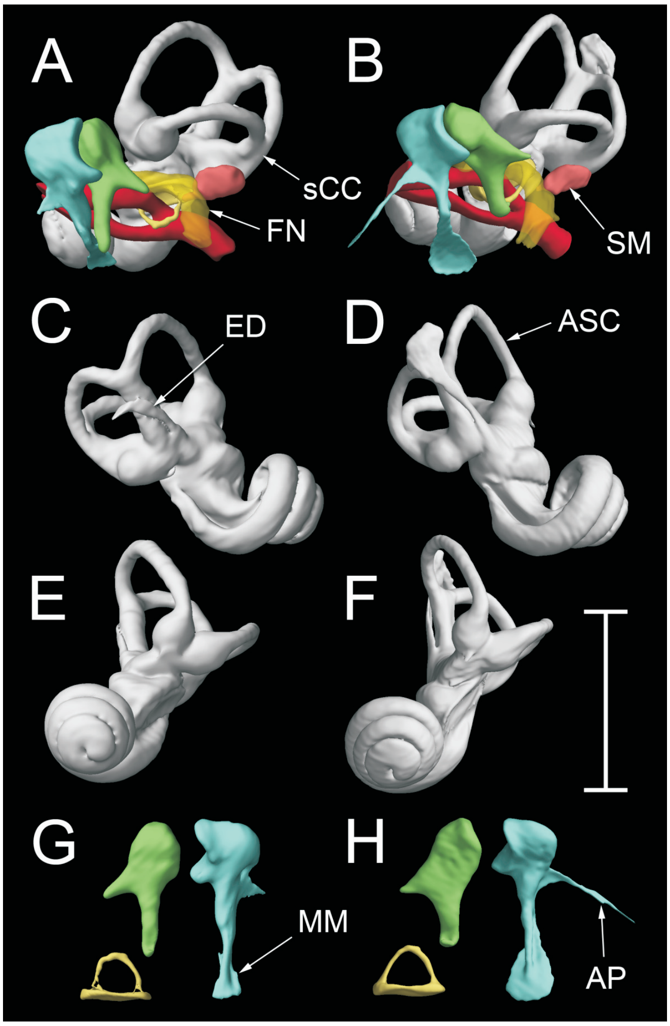

Figure 7. Reconstructions of left middle and inner ear structures of (**A**, **C**, **E**, **G**) the fossil specimen and (**B**, **D**, **F**, **H**) *Amblysomus hottentotus*. The *Amblysomus* reconstruction was of the right ear, but the images were laterally inverted to facilitate comparison. **A**, **B**, Ear structures seen from approximately lateral views; the ossicles in the fossil are disarticulated. **C**, **D**, Bony labyrinth, approximately medial view. **E**, **F**, Bony labyrinth, approximately anterior view. **G**, **H**, Malleus and incus, approximately medial views, and stapes, approximately dorsal view. Bony labyrinth = white; malleus = blue; incus = green; stapes = yellow; bony tubes for arteries = red. AP = anterior process of malleus; ASC = anterior semicircular canal; ED = bony tube for endolymphatic duct; FN = bony tube for facial nerve (translucent yellow); MM = manubrium of malleus; sCC = secondary crus commune; SM = bony tube for stapedius muscle (pink). Scale bar 3 mm.

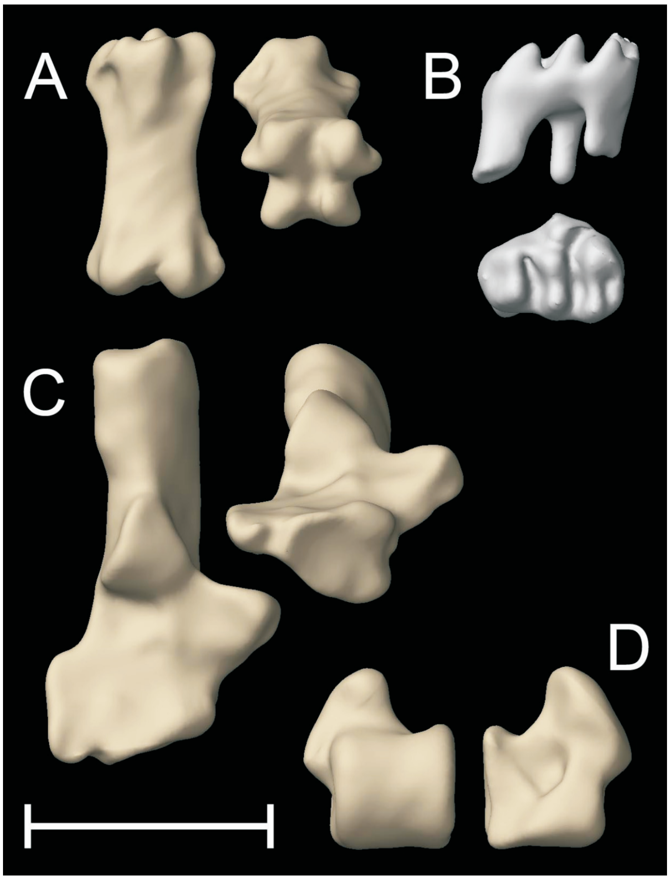

Figure 8. Reconstructions of some of the smaller fossils found in the matrix associated with the fossil golden mole skull. Two views are provided of each. **A**, rodent caudal vertebra; **B**, rodent molar; **C**, rodent calcaneum; **D**, golden mole talus. Scale bar 3 mm.

represent circumstantial evidence in favour of this identification:

1. It was found in the Ditsong National Museum of Natural History, where Broom's holotype *Proamblysomus* and *Chlorotalpa spelea* specimens are housed.
2. The reddish, silty, carbonate matrix still adhering to the specimen is compatible with it coming from Kromdraai, although similar deposits occur at both Sterkfontein and Bolt's Farm.
3. The fossil had been partially cleaned using a rotating abrasive wheel: Broom is known to have cleaned fossils with such a tool (Thackeray, J.F.: pers. comm., 2018).
4. The damage to its palate and teeth is consistent with the very brief existing descriptions by both Broom (1948) and De Graaff (1958), as cited in the Introduction.
5. The skull morphology is consistent with Broom's (1941) description of *Proamblysomus antiquus*, which both he and De Graaff (1961) believed this specimen likely represented (see later).
6. No similar skulls of fossil chrysochlorids have been described, to our knowledge, which our specimen could alternatively represent.

Considering these six points together, we believe that it is most parsimonious to conclude that this specimen is indeed Broom's missing skull. The identification of the species from which this comes is a separate issue, however, discussed in detail next.

Comparing the fossil to other golden moles

Broom (1948) believed that the fossil specimen which was subsequently lost was likely allied to *Proamblysomus*. He had previously described that genus from a single specimen, and could not be sure whether it had nine or ten teeth in the upper jaw (Broom 1941). The fossil examined here has nine, unlike most other known fossil golden moles which have ten: *Namachloris* (Pickford 2015), *Chlorotalpa spelea* (Asher 2010; Broom 1941), the fossil *Chrysochloris* species described from Langebaanweg (Asher & Avery 2010) and *Prochrysochloris* from Kenya (Butler 1984; Butler & Hopwood 1957). Nine teeth were, however, described in the fossil species *'Chrysotricha' hamiltoni* (De Graaff, 1958), which is now regarded as *Amblysomus* (Asher 2010; Butler 1978).

Among living golden moles, nine teeth are to be found in the closely-related amblysomines *Amblysomus* and *Neamblysomus*, and in the chrysochlorine *Calcochloris* (Meester 1974; Skinner & Smithers 1990). However, although tooth number has long been used in golden mole taxonomy (Broom 1907; Meester 1974; Skinner & Smithers 1990), it is well known that this is beset by difficulties based on variations in the number found in different individuals of the same species (Asher *et al*. 2010; Avery 1998; Bronner 1995; Ellerman *et al*. 1953). For example, *Neamblysomus gunningi* may have ten teeth in upper or lower jaws (Ellerman *et al*. 1953; Meester 1974). This also occurs, albeit very rarely, in *Amblysomus hottentotus* (Bronner 1995, 1996b), and Avery (1998) suggests that the same may be true of *N. julianae*, based on one specimen which had a small M_3 (Meester 1972). *Huetia* and *Chrysochloris* species typically have ten but may occasionally have nine teeth (Ellerman *et al*. 1953; Meester 1974). One must, then, be very cautious in using tooth number to align our fossil with one group or another, but the possession of just nine upper jaw teeth in our fossil specimen is at least suggestive of its possible affinities.

Calcochloris can be distinguished from *Amblysomus* and *Neamblysomus* species by its molariform first premolars (Bronner 1995; Meester 1974). Reconstructions of the upper jaws (Fig. 4) show that the alveolus of PM1 in *Calcochloris* is very similar in shape to the alveolus for PM2. In *Amblysomus*, the alveolus for PM1 has a much simpler, triangular shape. That of the fossil is intermediate between the two, but closer to *Amblysomus*. The two premolars remaining in the fossil skull are narrow in an anterior–posterior direction relative to their lateral width and in this respect they resemble those of *Calcochloris* more than those of *Amblysomus*, but it should be noted that both of these teeth have damaged cusps.

Malleus morphology varies greatly among golden mole genera, and has long been used for taxonomic purposes (Asher *et al*. 2010; Broom 1946, 1950; Forster Cooper 1928; Mason *et al*. 2006; Simonetta 1968; von Mayer *et al*. 1995). The fossil species examined here has relatively small mallei of 'freely mobile' morphology. This characteristic is shared by *Amblysomus*, *Neamblysomus*, *Calcochloris* and *Huetia* species (Mason 2003a,b; Mason *et al*. 2018; von Mayer *et al*. 1995). Middle and inner ear structures of the fossil species are very similar to those of *Amblysomus* and *Calcochloris* species, but *Calcochloris* has a slightly more elongated malleus head and articulation facet, and increased cochlear coiling (Mason *et al*. 2018). The malleus of the fossil species *Chlorotalpa spelea* is undescribed, but extant *Chlorotalpa* species have mallei which are much larger and clearly very different in morphology from that of our fossil specimen (Mason 2004).

Like all extant chrysochlorids, the specimen described here possessed a *m. stapedius* but apparently lacked a *m. tensor tympani*. The lack of the tensor muscle can be inferred from the convergence of the bony tubes for the stapedial and promontorial arteries beyond the oval window, which obliterates the fossa for the muscle belly which would normally lie in-between. The arteries did not converge in *Namachloris* and a tensor was interpreted as inhabiting the fossa between them (Mason *et al*. 2018). Pneumatization of the fossil skull by the middle ear cavity (Fig. 5) is a little more extensive than in *Amblysomus*, especially posterior to the roots of the zygomata. It is not as extensive as in *Calcochloris*, in which it penetrates the lateral skull wall well above the root of the zygomatic arch, and also invades the occipital condyles (Mason *et al*. 2018). Right and left middle ear cavities are continuous in the fossil via the pneumatized basisphenoid, a feature common to most extant golden moles but not the Palaeogene *Namachloris* (Mason 2016; Mason *et al*. 2018). The foramen ovale in *Amblysomus*, *Neamblysomus* and *Calcochloris* is in all cases well separated from the sphenorbital fissure (Asher *et al*. 2010), a feature apparently correlated with skull pneumatization (Mason *et al*. 2018), and this is also the case in the fossil described here. The inferior ramus of the stapedial artery appears to leave the skull through an opening confluent with the oval window. This is not the case in the amblysomines and *Calcochloris*, although it does occur in many other golden mole species including *Huetia* (Asher *et al*. 2010; Mason *et al*. 2018).

As well as teeth and middle ear characteristics, skull proportions have also been used to distinguish between golden moles (Bronner 1995, 1996a, b; De Graaff 1958; Meester 1974). Inspection of Figs 2 and 3 show that the skull of our fossil species is more similar in size and proportions to *Amblysomus hottentotus* than to *Calcochloris obtusirostris*. The fossil skull differs most notably from that of *Amblysomus* in the wider separation between zygomatic arch and orbital region and the more rounded contour of the dorsal aspect of the skull.

Cranial measurements from fossil golden moles (Table 2) were compared with equivalent measurements of extant species taken from Bronner (1995), focusing on the 'small malleus' chrysochlorids in the amblysomine genera *Amblysomus* and *Neamblysomus*, and the chrysochlorines *Calcochloris* and *Huetia* (Table 3). Greatest skull width and length measurements from our fossil were only minimally affected by damage to the skull, so should represent good estimates. Inspection of Table 3 shows that measurements for our fossil fall within or very close to the known size-ranges of several amblysomine species and subspecies. Notably, these include *A. hottentotus longiceps*, *A. septentrionalis* and *N. gunningi*, the southern African distributions of which come relatively close to Kromdraai (Mynhardt *et al*. 2015; Skinner & Smithers 1990). Given their collection site, the three *Amblysomus* specimens examined here were likely to be *A. hottentotus pondoliae,* which have similar skull dimensions but come from further afield. The fossil skull is markedly larger than those of *N. julianae*, *C. obtusirostris* and *H. leucorhinus*.

Broom (1941) originally distinguished *Proamblysomus* from *Amblysomus* based on its wider temporal region and more elongated bony external auditory meatus. The temporal region of our fossil is not as broad as what is shown in Broom's simple diagram (Fig. 9A). However, our fossil skull has a length:width ratio below any of the values for amblysomines computed from the mean length and width measurements in Table 3, except for the much smaller *Neamblysomus julianae*. In absolute terms, the fossil skull's width is above the average width of the majority of

Table 2. Comparison of measurements (in mm) and tooth counts of the skulls of fossil chrysochlorids from the Plio-Pleistocene of South Africa, and two extant species. Data for *Proamblysomus* and *Chlorotalpa* are from Broom (1941) and those for '*Chrysotricha*' are from De Graaff (1958). Broom measured 'width across the frontals' and De Graaff 'interorbital constriction': these measures have been included as 'mid-interorbital widths' in the table below although they may not represent precisely the same measurements. The remaining measurements and counts were made in the present study, from CT reconstructions.

	Proamblysomus antiquus	*Chorotalpa spelea*	'*Chrysotricha*' *hamiltoni*	Fossil specimen examined here	*Amblysomus hottentotus* (mean and range, *n* = 3)	*Calcochloris obtusirostris* (mean and range, *n* = 2)
Greatest skull length	*c.* 29	23.4	26.4	26.6	26.6 (26.4–26.9)	22.2 (21.9–22.5)
Greatest skull width	20.2	14.9	19.8	17.2	16.1 (15.5–16.5)	16.3 (16.1–16.4)
Length:width ratio	*c.* 1.44	1.57	1.33	1.55	1.66 (1.63–1.70)	1.36 (1.33–1.39)
Mid-interorbital width	8.4	7.2	7.7	8.3	8.3 (8.2–8.3)	7.2 (7.1–7.3)
Number of teeth in upper jaw	9 or 10 (uncertain)	10	9	9	9	9

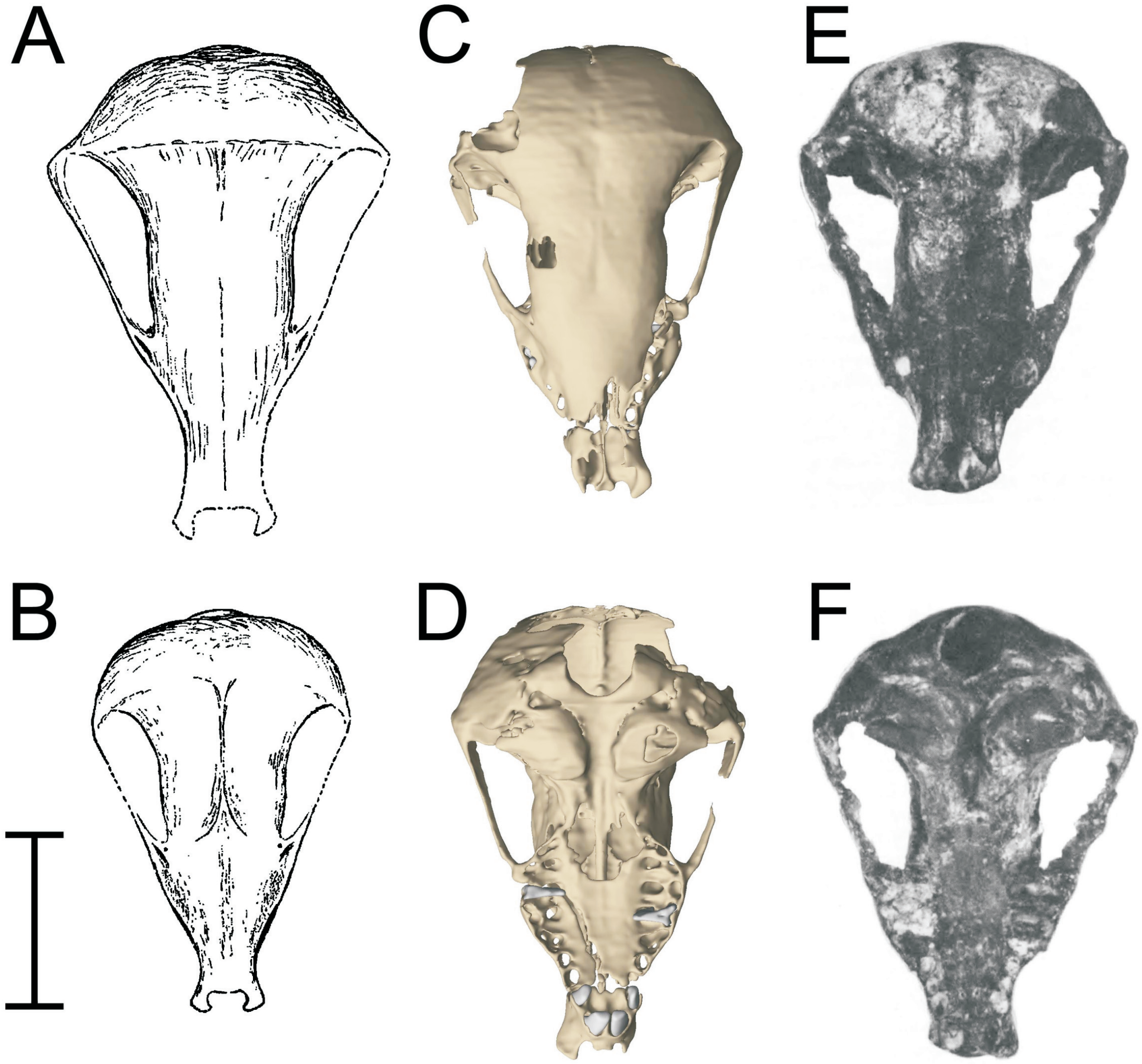

Figure 9. Gauteng and Makapansgat chrysochlorid skulls. **A**, Diagram based on the holotype of *Proamblysomus antiquus*, Ditsong National Museum of Natural History TM PAL 1573, from Broom (1941); **B**, Diagram based on the holotype of *Chlorotalpa spelea*, Ditsong National Museum of Natural History TM PAL 1572, from Broom (1941); **C**, **D**, reconstructions of the fossil species described herein; **E**, **F**, photographs of the holotype of *'Chrysotricha' hamiltoni*, Evolutionary Studies Institute, University of the Witwatersrand, MF.1, from De Graaff (1948). D and F are in ventral view; others are in dorsal view. Scale bar 10 mm. Yes. We obtained permission from both journals. Diagrams A & B are reproduced from Broom (1941) with kind permission of the Ditsong National Museum of Natural History, and E & F are reproduced from De Graaff (1948) with kind permission of *Palaeontologia africana*.

Table 3. Skull measurements of species and subspecies of extant, 'small malleus' golden moles, from Bronner (1995). Nomenclature has been updated after Bronner (2000) and Asher *et al*. (2010). Means for males and females were averaged; the ranges are for both sexes considered together. Length:width ratios were calculated from the mean values. Measurements from the fossil specimen described in the present paper are included for comparison.

	Greatest skull length (mm)	Greatest skull width (mm)	Length:width ratio	Mid-intraorbital width (mm)
Fossil specimen	26.6	17.2	1.55	8.3
Amblysomus corriae corriae	27.1 (25.3–28.9, *n* = 45)	15.7 (14.7–16.9, *n* = 45)	1.73	8.2 (7.5–8.8, *n* = 42)
Amblysomus c. devilliersi	27.0 (25.7–28.8, *n* = 16)	15.7 (15.2–16.6, *n* = 15)	1.72	8.0 (7.5–8.3, *n* = 16)
Amblysomus hottentotus hottentotus	26.2 (24.6–27.7, *n* = 46)	16.3 (15.1–17.7, *n* = 46)	1.61	8.1 (7.4–8.8, *n* = 45)
Amblysomus h. iris	25.4 (23.4–27.6, *n* = 19)	15.9 (14.9–17.9, *n* = 19)	1.60	8.3 (7.6–9.3, *n* = 16)
Amblysomus h. longiceps	28.7 (26.6–30.1, *n* = 49)	17.6 (16.3–19.4, *n* = 45)	1.63	9.1 (8.1–10, *n* = 46)
Amblysomus h. meesteri	27.5 (26.6–28.5, *n* = 5)	16.0 (15.3–16.6, *n* = 5)	1.72	7.9 (7.8–8.0, *n* = 5)
Amblysomus h. pondoliae	26.8 (24.9–29.4, *n* = 224)	16.8 (14.6–19.3, *n* = 233)	1.60	8.3 (7.0–9.0, *n* = 231)
Amblysomus marleyi	23.7 (22.4–24.7, *n* = 12)	15.0 (13.9–16.0, *n* = 12)	1.58	7.0 (6.5–7.5, *n* = 12)
Amblysomus robustus	29.8 (27.2–32.0, *n* = 21)	18.4 (16.6–20.4, *n* = 21)	1.62	9.5 (8.2–10.6, *n* = 21)
Amblysomus septentrionalis	28.6 (26.2–30.5, *n* = 41)	17.5 (16.1–19.5, *n* = 41)	1.63	9.1 (8.5–9.7, *n* = 41)
Neamblysomus gunningi	28.0 (27.0–29.3, *n* = 17)	17.0 (15.9–18.2, *n* = 17)	1.65	8.0 (7.6–8.7, *n* = 17)
Neamblysomus julianae	22.9 (21.8–23.6, *n* = 15)	15.7 (14.7–16.7, *n* = 15)	1.46	7.2 (6.4–7.8, *n* = 15)
Calcochloris obtusirostris	22.1 (19.0–24.2, *n* = 38)	15.8 (13.8–16.8, *n* = 41)	1.40	7.2 (6.2–7.7, *n* = 41)
Huetia leucorhinus	22.0 (19.5–23.1, *n* = 8)	15.6 (12.9–16.9, *n* = 8)	1.41	7.7 (6.8–8.4, *n* = 9)

amblysomine species and subspecies. The bony external meatus of the fossil also narrows distally, giving it the appearance of elongation, so overall our fossil specimen does appear to be broadly consistent with the brief description of the *Proamblysomus antiquus* holotype. De Graaff (1958) distinguished '*Chrysotricha*' (Fig. 9E,F), now regarded as a species of *Amblysomus* (Asher 2010; Butler 1978), from *Proamblysomus* based on its shorter, wider muzzle and more curved dental arch. Owing to the damage to the nasal region of the specimens in question and the poor quality of the available illustrations, we find it difficult to place our skull closer to *Proamblysomus* or '*Chrysotricha*' based on these characteristics.

Avery (1998) pointed out that the incomplete preparation of Broom's specimens of both *Proamblysomus antiquus* (Fig. 9A) and *Chlorotalpa spelea* (Fig. 9B) makes it very hard to be certain of their taxonomic identity. Further work on these specimens, potentially including CT reconstruction, is clearly needed in order to establish whether *Proamblysomus* really deserves generic distinction from extant groups and, if so, whether the fossil specimen described here should also be assigned to *Proamblysomus*.

Taphonomy and age of the fossil specimen

Several bones from small mammals were identified within the matrix associated with the fossil skull, mostly within the braincase. As well as a molar believed to come from *Steatomys*, there was a calcaneum and a caudal vertebra of a rodent, possibly from the same species. *Steatomys* is known from a number of cave breccia deposits in Gauteng, ranging in age from 4.5 Ma until the Recent (Avery 1998, 2000, 2001). The chrysochlorid talus could be from the same individual as the skull. The skull may therefore have been from an owl pellet, also containing the remains of other recent meals. De Graaff (1961) did not find any golden mole specimens in the Pleistocene owl pellets from the Transvaal cave system which he examined, attributing this to the fact that, being fossorial, golden moles rarely fall prey to owls. He suggested that his Makapansgat specimen may instead have been dug up by australopithecines (De Graaff 1958). However, some extant golden moles do show above-ground activity, and remains have been found in owl pellets (Hickman 1990).

If it came from Kromdraai, the age of the chrysochlorid specimen examined here would be Plio-Pleistocene.

Pickford (2013) estimated that the Kromdraai A deposits are aged about 1.8–1.6 Ma, whereas Braga *et al*. (2017) summarized the situation at Kromdraai as 'problematic', partly because there are two deposits (Kromdraai A and Kromdraai B), but also because the deposits at Kromdraai B comprise several different stratigraphic levels (members). Unfortunately, we are unable to specify the age of this fossil specimen with any precision, but its association with *Steatomys* is compatible with it being from the late Pliocene or early Pleistocene.

CONCLUSION

Evidence suggests that the fossil skull described here is the missing Kromdraai specimen briefly referred to by Broom (1948) and De Graaff (1958). Dentition and middle ear morphology of this fossil show similarities with *Amblysomus*, *Neamblysomus* and *Calcochloris* species, while skull measurements align the fossil more clearly with members of the first two genera. A more detailed analysis, including other fossil specimens, would be required to determine whether this specimen is sufficiently distinct from extant amblysomine species to be distinguished as *Proamblysomus*.

We thank Mirriam Tawane and Lazarus Kgasi for authorizing the temporary loan of the fossil. M.P. thanks the Muséum National d'Histoire Naturelle for support and Sorbonne Université – CR2P, MNHN, CNRS, UPMC – Paris VI, for financial support (S. Crasquin, D. Gommery). We thank Frank Sénégas for identifying the rodent tooth that was found inside the skull, the Cambridge Biotomography Centre for the use of their scanner, and Andrew Gee and Graham Treece for their help and advice regarding the use of Stradwin. All images reconstructed from Natural History Museum specimens are shown courtesy of the Trustees of the Natural History Museum, London, and we thank Paula Jenkins and Roberto Portela Miguez for facilitating the original loan. Finally, we thank the two reviewers for some insightful comments which have substantially improved the paper. This work was partially funded by a National Research Foundation grant to N.C.B.

---

§ORCID iDs

M.J. Mason: orcid.org/0000-0001-7845-0720
N.C. Bennett: orcid.org/0000-0001-9748-2947

REFERENCES

ASHER, R.J. 2010. Tenrecoidea. **In**: Werdelin L. & Sanders, W.J. (eds), *Cenozoic Mammals of Africa*, 99–106. Berkeley, University of California Press.

ASHER, R.J. & AVERY, D.M. 2010. New golden moles (Afrotheria, Chrysochloridae) from the Early Pliocene of South Africa. *Palaeontologia Electronica* **13**(1 (3A)), 1–12.

ASHER, R.J. & LEHMANN, T. 2008. Dental eruption in afrotherian mammals *BMC Biology* **6**(14); DOI: 10.1186/1741-7007-6-14

ASHER, R.J., MAREE, S., BRONNER, G., BENNETT, N.C., BLOOMER, P., CZECHOWSKI, P., MEYER, M. & HOFREITER, M. 2010. A phylogenetic estimate for golden moles (Mammalia, Afrotheria, Chrysochloridae). *BMC Evolutionary Biology* **10**, 69.

AVERY, D.M. 1998. An assessment of the lower Pleistocene micromammalian fauna from Swartkrans Members 1–3, Gauteng, South Africa. *Geobios* **31**, 393–414.

AVERY, D.M. 2000. Notes on the systematics of micromammals from Sterkfontein, Gauteng, South Africa. *Palaeontologia africana* **36**, 83–90.

AVERY, D.M. 2001. The Plio-Pleistocene vegetation and climate of Sterkfontein and Swartkrans, South Africa, based on micromammals. *Journal of Human Evolution* **41**, 113–132.

BRAGA, J., THACKERAY, F., BRUXELLES, L., DUMONCEL, J. & FOURVEL, J.-B. 2017. Stretching the time span of hominin evolution at Kromdraai (Gauteng, South Africa): recent discoveries. *Comptes Rendus Palevol* **16**, 58–70.

BRONNER, G.N. 1995. Systematic revision of the golden mole genera *Amblysomus*, *Chlorotalpa* and *Calcochloris* (Insectivora: Chrysochloromorpha; Chrysochloridae). Ph.D. thesis, University of Natal, Durban.

BRONNER, G.N. 1996a. Geographic patterns of morphometric variation in the Hottentot golden mole, *Amblysomus hottentotus* (Insectivora: Chrysochloridae). A multivariate analysis. *Mammalia* **60**(4), 729–752.

BRONNER, G.N. 1996b. Non-geographic variation in morphological characteristics of the Hottentot golden mole, *Amblysomus hottentotus* (Insectivora: Chrysochloridae). *Mammalia* **60**(4), 707–728.

BRONNER, G.N. 2000. New species and subspecies of golden mole (Chrysochloridae: *Amblysomus*) from Mpumalanga, South Africa. *Mammalia* **64**(1), 41–54.

BROOM, R. 1907. On some new species of *Chrysochloris*. *Annals and Magazine of Natural History*, (7)**19**, 262–268.

BROOM, R. 1941. On two Pleistocene golden moles. *Annals of the Transvaal Museum* **20**, 215–216.

BROOM, R. 1946. Some new and some rare golden moles. *Annals of the Transvaal Museum* **20**(4), 329–335.

BROOM, R. 1948. Some South African Pliocene and Pleistocene mammals. *Annals of the Transvaal Museum* **21**(1), 1–38.

BROOM, R. 1950. Some further advances in our knowledge of the Cape golden moles. *Annals of the Transvaal Museum* **21**, 234–241.

BUTLER, P.M. 1978. Insectivora and Chiroptera. **In**: Maglio, V.J. & Cooke, H.B.S. (eds), *Evolution of African Mammals*, 56–68. Cambridge (Mass.) and London, Harvard University Press.

BUTLER, P.M. 1984. Macroscelidea, Insectivora and Chiroptera from the Miocene of East Africa. *Palaeovertebrata* **14**(3), 117–200.

BUTLER, P.M. & HOPWOOD, A.T. 1957. Insectivora and Chiroptera from the Miocene rocks of Kenya Colony. *Fossil Mammals of Africa* **13**, 1–35.

DE GRAAFF, G. 1958. A new chrysochlorid from Makapansgat. *Palaeontologia africana* **5**, 21–27.

DE GRAAFF, G. 1961. A preliminary investigation of the mammalian microfauna in Pleistocene deposts of caves in the Transvaal system. *Palaeontologia africana* **7**, 59–118.

ELLERMAN, J.R., MORRISON-SCOTT, T.C.S. & HAYMAN, R.W. 1953. *Southern African Mammals 1758 to 1951: A Reclassification*. London, Trustees of the British Museum.

FORSTER COOPER, C. 1928. On the ear region of certain of the Chrysochloridae. *Philosophical Transactions of the Royal Society of London B* **216**, 265–283.

GINOT, S., HAUTIER, L., MARIVAUX, L. & VIANEY-LIAUD, M. 2016. Ecomorphological analysis of the astragalo-calcaneal complex in rodents and inferences of locomotor behaviours in extinct rodent species. *PeerJ* **4**: e2393; DOI: 10.7717/peerj.2393

HICKMAN, G.C. 1990. The Chrysochloridae: studies toward a broader perspective of adaptation in subterranean mammals. **In**: Nevo, E. & Reig, O.A. (eds), *Evolution of Subterranean Mammals at the Organismal and Molecular Levels*, 23–48. New York, Wiley-Liss.

LUCKETT, W.P. 1993. An ontogenetic assessment of dental homologies in therian mammals. **In**: Szalay, F.S., Novacek, M J. & McKenna, M.C. (eds), *Mammal Phylogeny: Mesozoic Differentiation, Multituberculates, Monotremes, Early Therians, and Marsupials*, 182–204. New York, Springer Science+Business Media.

MASON, M.J. 2003a. Bone conduction and seismic sensitivity in golden moles (Chrysochloridae). *Journal of Zoology* **260**, 405–413.

MASON, M.J. 2003b. Morphology of the middle ear of golden moles (Chrysochloridae). *Journal of Zoology* **260**, 391–403.

MASON, M.J. 2004. Functional morphology of the middle ear in *Chlorotalpa* golden moles (Mammalia, Chrysochloridae): predictions from three models. *Journal of Morphology* **261**(2), 162–174.

MASON, M.J. 2016. Internally coupled ears in living mammals. *Biological Cybernetics* **110**(4), 345–358.

MASON, M.J., BENNETT, N.C. & PICKFORD, M. 2018. The middle and inner ears of the Palaeogene golden mole *Namachloris*: a comparison with extant species. *Journal of Morphology* **279**, 375–395.

MASON, M.J., LUCAS, S.J., WISE, E.R., STEIN, R.S. & DUER, M.J. 2006. Ossicular density in golden moles (Chrysochloridae). *Journal of Comparative Physiology A: Neuroethology, Sensory, Neural, and Behavioral Physiology* **192**(12), 1349–1357.

MEESTER, J. 1972. A new golden mole from the Transvaal (Mammalia: Chrysochloridae). *Annals of the Transvaal Museum* **28**(4), 35–46.

MEESTER, J. 1974. Family Chrysochloridae. **In**: Meester, J. & Setzer, H.W. (eds), *The Mammals of Africa: an Identification Manual*, 1–7. Washington DC, Smithsonian Institution Press.

MYNHARDT, S., MAREE, S., PELSER, I., BENNETT, N.C., BRONNER, G.N., WILSON, J.W. & BLOOMER, P. 2015. Phylogeography of a morphologically cryptic golden mole assemblage from south-eastern Africa. *PLOS ONE* **10**(12), e0144995.

O'LEARY, M.A., BLOCH, J.I., FLYNN, J.J., GAUDIN, T.J., GIALLOMBARDO, A., GIANNINI, N.P., GOLDBERG, S.L., KRAATZ, B.P., LUO, Z.-X., MENG, J., NI, X., NOVACEK, M.J., PERINI, F.A., RANDALL, Z.S., ROUGIER, G.W., SARGIS, E.J., SILCOX, M.T., SIMMONS, N.B., SPAULDING, M., VELAZCO, P.M., WEKSLER, M., WIBLE, J.R. & CIRRANELLO, A.L. 2013. The placental mammal ancestor and the Post-K-Pg radiation of placentals. *Science* **339**(6120), 662–667.

PICKFORD, M. 2013. The diversity, age, biogeographic and phylogenetic relationships of Plio-Pleistocene suids from Kromdraai, South Africa. *Annals of the Ditsong National Museum of Natural History* **3**, 1–32.

PICKFORD, M. 2015. Late Eocene Chrysochloridae (Mammalia) from the Sperrgebiet, Namibia. *Communications of the Geological Survey of Namibia* **16**, 153–193.

POCOCK, T.N. 1987. Plio-Pleistocene fossil mammalian microfauna of southern Africa – a preliminary report including description of two new fossil muroid genera (Mammalia: Rodentia). *Palaeontologia africana* **26**(7), 69–91.

SIMONETTA, A.M. 1968. A new golden mole from Somalia with an appendix on the taxonomy of the family Chrysochloridae (Mammalia, Insectivora). *Monitore Zoologico Italiano (N,S,)* **2** (supplement), 27–55.

SKINNER, J.D. & SMITHERS, R.H.N. 1990. *The Mammals of the Southern African Subregion*. Pretoria, University of Pretoria.

VAN HOEPEN, E. & VAN HOEPEN, H. 1932. Vrijstaatse wilde varke. *Palaeontologiese Navorsing van die Nasionale Museum*, *Bloemfontein* **2**(4), 39–62.

VON MAYER, A., O'BRIEN, G. & SARMIENTO, E.E. 1995. Functional and systematic implications of the ear in golden moles (Chrysochloridae). *Journal of Zoology* **236**, 417–430